Construction and Optimization of shRNA/siRNA Lentivral Vectors for microRNA-486-5p Using miR-30/451 and miRNA Sponges

Wenlun Wang[1, 2], Feng Zhang[1], Lu Min[2], Xiaomin Wu[2], Zixuan Yu[2], Junhao Yang[1], Xiaoqing Cai[1], Qing Lin[1], Yanmei Fan[1], Jun Xu[1], Linghai Zeng[1], Qian Hu[1], Dongyi Zhang[2], Lingyun Zhu[2, *]

[1]Department of Food Science and Engineering, Moutai Institute, Renhuai 564507, China

[2]Department of Biology and Chemistry, College of Sciences, National University of Defense Technology, Changsha 410073, China

Abstract: By analyzing the hairpin structure of miR-486, it was found that the mature sequences of miR-486-5p and miR-486-3p are complementary. For this reason, it is probably the greatest challenge to express miR-486-5p using a lentiviral expression vector in C2C12 cells. Thus, we constructed shRNA/siRNA lentiviral expression vectors for microRNA-486-5p based on miR-30/451 and miRNA sponges. Oligonucleotide sequences (miR-486-5p TuD (tough decoy RNAs), miR-486-5p sponge, miR-486-5p-shRNA30 and miR-486-5p-shRNA451) were digested and cloned into the PLV-U6-MCS vector to generate U6-driven expression cassettes for mmu-miR-486-5p, and these vectors, including anti-miR-486-5p TuD, anti-miR-486-5p sponge, miR-486-5p-shRNA30 and miR-486-5p-shRNA451, were assessed by sequencing. The lentivirus vector was packaged in 293T cells according to the manufacturer's instructions. Subsequently, C2C12 cells were infected using a lentivirus for the expression of miR-486-5p, and this lentivirus of PLV-U6-MCS served as a control. qRT-PCR analysis showed that anti-miR-486-5p TuD and the anti-miR-486-5p sponge decreased the expression level of miR-486-5p in C2C12 cells by 0.5-fold and 0.7-fold, respectively. Additionally, miR-486-5p-shRNA30 and miR-486-5p-shRNA451 upregulated the expression level of miR-486-5p in C2C12 cells by 15-fold and 3-fold, respectively. However, the expression level of miR-486-3p was increased up to 1000-fold in C2C12 cells containing the miR-486-5p-shRNA30 lentivirus, while other lentiviruses only led to 3-fold increases compared with the miR-486–5p-shRNA30 lentivirus in C2C12 cells. Additionally, western blot and gray density analysis demonstrated that the expression levels of AKT, and pAKT, ERK1/2 and pERK1/2, and Snail were upregulated (approximately 1.20-fold to 1.33-fold and 1.05-fold to 1.20-fold, respectively) in C2C12 cells infected with the anti-miR-486-5p TuD lentivirus and anti-miR-486-5p sponge lentivirus and downregulated (approximately 0.63–0.96 times and 0.72–0.92 times, respectively) in C2C12 cells infected with the miR-486-5p-shRNA30 lentivirus and miR-486-5p-shRNA451 lentivirus. In summary, anti-miR-486-5p TuD, which dramatically reduced the expression level of miR-486-5p and upregulated endogenous protein levels in C2C12 cells, was superior to the anti-miR-486-5p sponge in terms of interference expression of miR-486-5p.

Funding: Guizhou Provincial Basic Research Program (Natural Science), (No. QiankeHeJiChu-ZK[2024]-YiBan-659);
The Youth Science and Technology Talent Growth Project of Guizhou Province Education Department (No. QianJiaoKe[2024]262);
Zunyi Technology and Big Data Bureau, Moutai Institute Joint Science and Technology Research and Development Project, grant number: (ZSKHHZ[2021]No.332);
The Natural Science Foundation of Hunan Province, grant number: (CX20190003);
The Research Foundation for Scientific Scholars of Moutai Institute, grant number: (mygccrc [2023]011).

*Corresponding author: Lingyun Zhu, lingyunzhu@nudt.edu.cn

Received: 21 August 2024; Accepted: 29 November 2024; Published Online: 4 July 2025 http://www.lifescitech.org

miR-486-5p-shRNA451, which did not lead to substantial expression of miR-486-3p and remarkably downregulated endogenous protein levels in C2C12 cells, was better than miR-486-5p-shRNA30 for overexpression of miR-486-5p. These results suggested that anti-miR-486-5p TuD and miR-486-5p-shRNA451 provide a simple way to build long-term effective overexpression or interference of miR-486-5p, to study miRNA function in C2C12 and mice, and to create a potential diagnostic method based on materials for diseases caused by miRNA deregulation.

Keywords: miR-486; miR-486-5p; siRNA and shRNA Vector; C2C12; Lentivirus Vector; Tough Decoy (TuD) RNA; miR-486 spOnge; miR30-based and miR451-based shRNA Vector

DOI: 10.57237/j.life.2025.01.002

1 Introduction

microRNAs (miRNAs) comprise a large family of 20–22 nt nucleotide-long noncoding RNAs that have emerged as major posttranscriptional regulators of gene expression in animals and plants [1, 2]. Canonical miRNA function carefully regulates gene expression by sponging specific mRNA targets in the 3′ untranslated region (3′UTR), promoting their degradation and/or translational inhibition in cells, and participating in the progression of cell fate and origin development, such as cell apoptosis, cell proliferation, and cell differentiation [3, 4]. In addition, there are 7 categories of unconventional miRNA functions [5]: pri-miRNAs coding for peptides, miRNAs interacting with non-AGO proteins, miRNAs activating Toll-like receptors, miRNAs upregulating protein expression, miRNAs targeting mitochondrial transcripts, miRNAs directly activating transcription, and miRNAs targeting nuclear ncRNAs. However, one known miRNA, which may modulate the expression of thousands of target genes in a broad range of cells or organisms and may have substantial effects on regulatory networks of gene expression, exhibits multiple biological functions in cell development [6]. Therefore, overexpression or inhibition of miRNA is one of the most promising means by which to investigate its biological function in cells or animals.

miRNA-486 is a 20–22-nucleotide noncoding RNA sequence localized to chromosome 8q11.42 in mice or 8q11.21 in humans and is a muscle-enriched miRNA [7-9]. miR-486, which is directly regulated by MyoD, myogenin, MYF5, SRF (serum response factor) and MRTF-A (myocardin-related transcription factor-A), is encoded by intron 40 of the ankyrin-1 gene and is conserved in mammals [9, 10]. Currently, miR-486 negatively modulates the expression of PTEN (phosphatase and tensin homolog), FOXO1 (forkhead boxO1), DOCK3 (dedicator of cytokinesis 3), KIAA1199 and TENM1 (teneurin transmembrane protein 1), in turn positively enhancing the PI3K/Akt and ERK (extracellular-signal-regulated kinase) signaling pathways in cardiac, skeletal muscle cells and carcinoma cells [9, 11-13]. Furthermore, miR-486-5p suppresses cancer migration and invasion and regulates EMT (epithelial–mesenchymal transition) in prostate cancer by targeting Snail to inversely facilitate its expression [14]. However, accumulating evidence [7, 9] and the NCBI database have demonstrated that the mature sequence of miR-486-5p is complementarily paired with miR-486-3p (Figure 1). For this reason, it is very challenging to study the function of miR-486-5p in cells and animals. The question remains not only can miR-486-5p be overexpressed using a lentivirus vector but also whether it induces the significant expression of miR-486-3p, which is particularly important for establishing stable expression of miR-486-5p shRNA or siRNA cell lines.

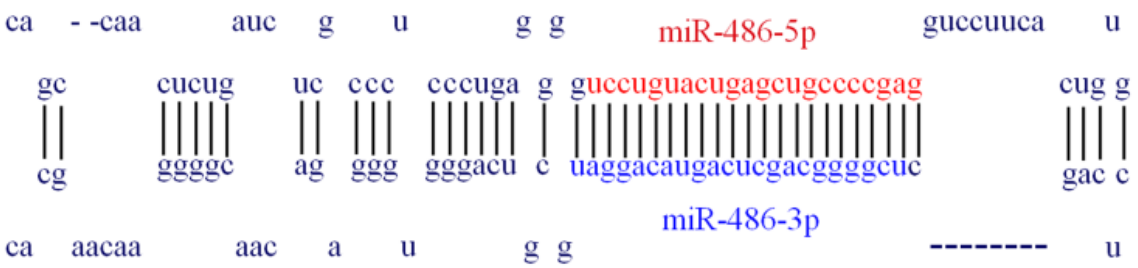

Figure 1 The sequence of the stem-loop structure of miR-486.

In recent years, numerous miRNA overexpression vectors have been constructed based on the hairpin structure of miR-30, which depends on the miRNA canonical pathway to yield a mature miRNA [15-17], such as miR-30 [16, 17] and miR-489 [18]. With an increased understanding of miRNA structure and biological function, it has been observed that noncanonical pathways of miRNA biogenesis contain Drosha-independent pathways (Mirtont, snoRNA-derived, tRNA-derived, shRNA-derived, pre-siRNA-derived) and Dicer-independent pathways (AGO-dependent and tRNaseZ-dependent pathways) [19-21]. In the AGO-dependent pathway, the hairpin structure of miR-451 is cleaved by Drosha to produce the pre-miR-451 hairpin, which is too short to be cleaved by Dicer and instead directly enters Ago2 (Argonaute2), and the latter cleaves the 3' arm of the hairpin to generate a product that is further resected by the PARN exonuclease to produce the mature miRNA (miR-451) [21-24]. With increasing recognition of an approach that constructs miRNA overexpression vectors, researchers have designed and developed a set structure of pre-miRNA-like shRNA based on miR-451, AGO-dependent pathways and PARA to express miRNAs in cells, such as miR-451 [25-31]. In addition, a miRNA siRNA expression vector was established based on the sponge mechanisms. The siRNA expression vector of miRNA was constructed by a commonly used method that clones multiple oligonucleotide sequences containing tandem "bulged" miRNA binding motifs (at least six repeats) into a target plasmid [32] to achieve knockdown of miRNA expression in cells, such as miR-486. Additionally, it has been shown that TuD RNA (tough decoy RNA) [33] adenovirus and lentivirus vectors also interfere with miRNA expression in cells, such as miR-140-3p and miR-140-5p [34], miR-17-92 [35], miR-203 [36], miR-122 and let-7 [37]. Taken together, overexpression and knockdown lentivirus vectors of mmu-miR-486-5p were established based on miR-30/451 and miRNA sponges, respectively, and then simultaneously, the expression level of mmu-miR-486-5p was assessed and its effects on the expression levels of Snail, ERK1/2, phosphorylation of ERK1/2 (p-ERK1/2), AKT and phosphorylation of Akt (p-Akt) were validated in C2C1 cells.

2 Materials and Methods

2.1 Cell Culture

HEK-293T and C2C12 cells were purchased from American Type Culture Collection (ATCC) and conserved in our laboratory. HEK-293T and C2C12 were cultured in growth medium (containing Dulbecco's modified Eagle's medium (DMEM, Hyclone, Thermo Fisher Scientific), 10% fetal bovine serum (FBS, Gibco, Grand Island, NY, USA), 100 IU/mL P/S (penicillin/streptomycin)). To induce C2C12 differentiation, cell growth medium was replaced with Differentiation medium (containing DMEM, 2% heat-inactivated horse serum (Gibco, Grand Island, NY, USA), 100 IU /mL P/S (penicillin/streptomycin)) when C2C12 cell confluence reached 90%. All those were cultured at 37 ℃ with 5% CO_2 in a humid atmosphere.

2.2 Plasmid Construction, Lentivirus Production and Infection of Target Cells

Plasmid construction: Plasmid construction was performed according to standard methods as described previously [16, 38-40]. We briefly described this process in the paper (Figure 2). The PLV-U6-MCS (Multiple cloning site include XbaI and PstI sites) are both a lentiviral empty vector with GFP, U6 were constructed as previously describe [40, 41], and were purchased from VectorBuilder and preserved in our laboratory. Oligonucleotide sequences, listed in Supplementary Table 1, were synthesized by General Biological System (Anhui) Co., Ltd. and cloned into the PLV-U6-MCS vector to generate U6-driven expression cassettes for expression of miR-486-5p shRNA or siRNA. siRNA miR-486-5p sequences of oligonucleotides was designed based on miRNA sponge, TuD RNAs (tough decoy RNAs,) sponge which contains two single-stranded miRNA-binding sites (here, for miR-486-5p) [34, 37, 42] and 6 repeated sponges target sites for miR-486-5p which includes six tandem "bulged" miR-486-5p-binding motifs [32], respectively. siRNA miR-486-5p sequences was digested, purified and ligated into XbaI and PstI sites of PLV-U6-MCS to make Anti-miR-486-5p TuD and Anti-miR-486-5p sponge plasmid. shRNA miR-486-5p sequences of oligonucleotides was designed based on miR-30/451 short hairpin RNA (shRNA) cassettes which contains mature miR-486-5p sequences [15, 25, 26, 43]. shRNA miR-486-5p sequences was acquired by digesting, purifying and inserted into XbaI and PstI sites of PLV-U6-MCS to generate miR-486-5p-shRNA30 and

miR-486-5p-shRNA451 vector.

Table 1 Complete synthesized oligonucleotide sequences used in this paper

Oligonucleotides	Sequence (5` to 3`)
miR-486-5p TuD	GCTCTAGAGACGGCGCTAGGATCATCAACCTCGGGGCAGCTAGCTCAGTACAG-GACAAGTATTCTGGTCACAGAATACAACCTCGGGGCAGCTAGCTCAGTACAGGACAA-GATGATCCTAGCGCCGTCTTTTTTCTGCAGAACG
miR-486-5p sponge	GCTCTAGACTCGGGGCGACCAGTACAGGAatccgtaCTCGGGGCGACCAGTACAGGAatccg-taCTCGGGGCGACCAGTACAGGAatccgtaCTCGGGGCGACCAGTACAGGAatccg-taCTCGGGGCGACCAGTACAGGAatccgtaCTCGGGGCGACCAGTACAGGAatccg-taCTCGGGGCGACCAGTACAGGATTTTTTCTGCAGAACG
miR-486-5p -shRNA30	GCTCTAGAGAAGGTATATTGCTGTTGACAGTGAGCGTCCTGTACTGAGCTGCCCCGAGTAG-TGAAGCCACAGATGTACTCGGGGCAGCTCAGTACAGGATGCCTACTGCCTCGGTTTTTCTG-CAGAACG
miR-486-5p -shRNA451	GCTCTAGAGCACTTGGGAATGGCAAGGTCCTGTACTGAGCTGCCCCGAGAGGGG-CAGCTCAGTACAGGCTCTTGCTATACCCAGAAAATTTTTCTGCAGAACG

Restriction sites are underlined, such as XbaI site is TCTAGA, PstI site is CTGCAG.

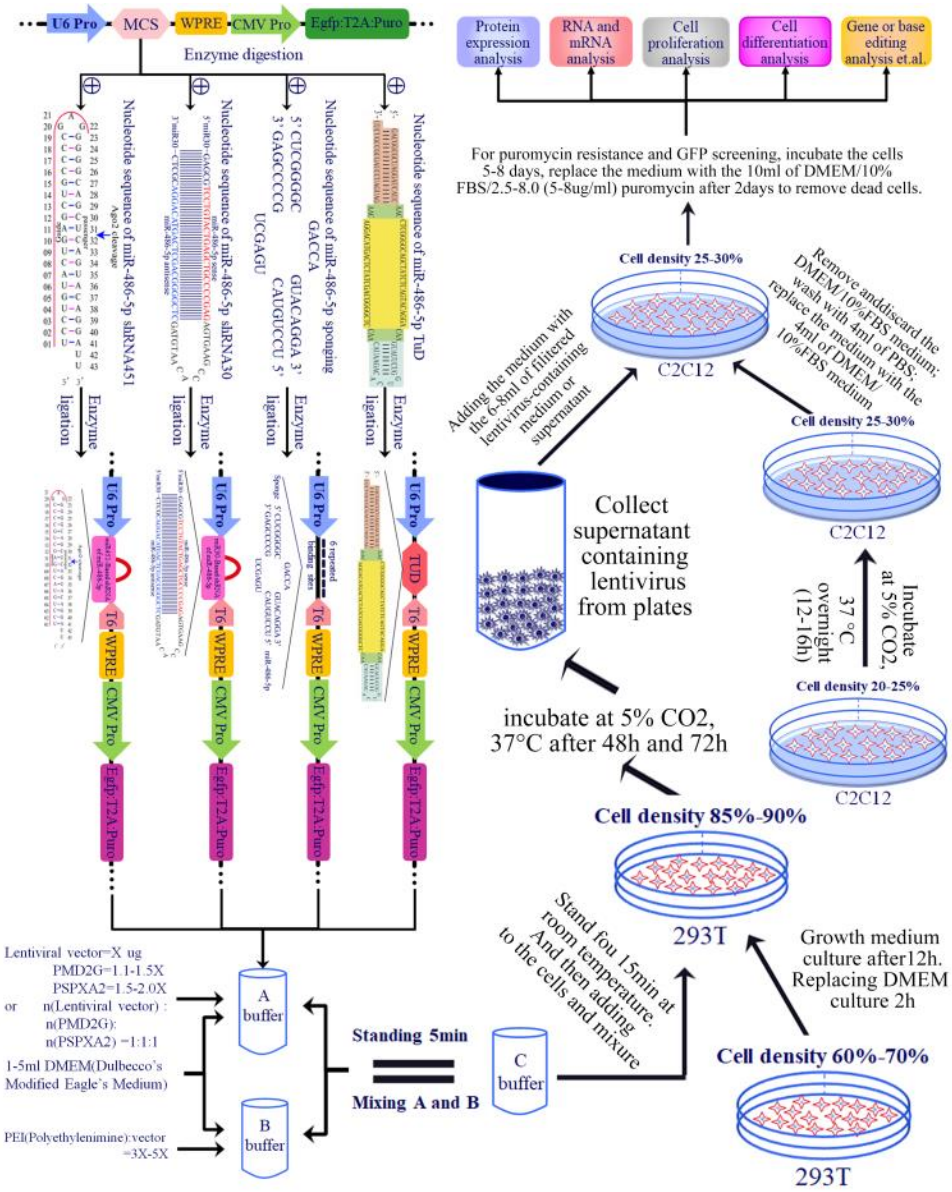

Figure 2 The process of Plasmid construction, lentivirus production and infection of target cells

Lentivirus production and purification: A detailed description of the Lentivirus production is beyond the scope of this article, and more detail is given in reference [44-47]. We briefly described this process in the paper (Figure 2). For lentivirus production, 2.5 × 106 HEK293T cells plated 10-cmd dishes in 10ml of growth medium. After 12-24h, cells were transfected with plasmid DNA transfection mix (30 μg of total DNA; psPAX2 packaging plasmid: pMD2.G envelope plasmid: target plasmid ratio = 1:1:1 (wt/wt/wt)) and 10ug of miR-486-5p shRNA, siRNA or control plasmid using PEI (polyethyleneimine, Roche, (1:2.5-5 (wt/wt) = total plasmid DNA:PEI ratio). 8-12h later media was switched with 10ml/plate of fresh medium. Supernatants were collected 48-72h after transfection, and passed through 0.45 μm filter and centrifuged at 3000g for 5min at 4 ℃ in RT (Thermo fisher). To concentrate virus, 40ml of supernatant was centrifuged at 26 000 r.p.m. for 2 h at 4 ℃ in RC6 Plus (Thermo fisher). Pellets were resuspended in 100 μl of DMEM at 4 ℃ overnight.

Infection of the C2C12 cells: A detailed description of the Lentivirus production is beyond the scope of this article, and more detail is given in reference [44, 48-50]. We briefly described this process in the paper (Figure 2). Adding ~0.5-1 × 105 C2C12 cells in 2.5ml of growth medium to a new 6-well tissue culture dish at 25–35% confluence, and place the dish in a humidified 5% CO_2 incubator overnight. And then, the growth medium was replaced with 2.5 ml transduction medium mixture per well containing 30ul lentivirus (calculated MOI=10), 2ul polybrene ((from a 10-mg/mL 1,000 × stock solution) and 2.468ml fresh medium, and centrifuge the 6-well plate at 3000 r.p.m for 30min at 37 ℃. After 24-48h, the medium was switched with 2.5ml growth medium including Puromycin (2-5ug/ml) and return the 6-well plate to the incubator for 24-48h. The stable expression of miR-486-5p shRNA or siRNA cell lines were established and selected in our laborious using GFP and Puromycin, and were used to analyze the expression level of miR-486-5p and cell function in C2C12 cells.

2.3 RNA Extraction and Quantitative Real-time PCR (qRT-PCR)

Total RNA was isolated from cultured cells (C2C12) using TRIzol Reagent (Thermo Fisher Scientific) according to the manufacturer's protocol. RNA concentration was evaluated with Nanodrop. After subsequently DNAse treatment, complementary DNA (cDNA) was generated using miRNA 1st Stand cDNA Synthesis Kit (by stem-loop) and HiScript III 1st Strand cDNA Synthesis Kit according to the manufacturer (Vazyme, China).

Expression of mature miRNAs was determined by SYBR qPCR Master Mix Kit (ChamQ Universal SYBR qPCR Master Mix) using miRNA-specific looped RT-primers as recommended by the manufacturer (Vazyme, China), and U6 snRNA was used as an internal control. cDNA was then used for quantitative PCR (qPCR) done with LightCycler 480 (Roche) and run in LC480 for 50 cycles. Stem-loop primer sequence for qRT-PCR was performed according to standard methods as described previously [51]. All primer was listed in Supplementary Table 2, and synthesized by General Biological System (Anhui) Co., Ltd. All samples were duplicated.

Table 2 designed RT stem-loop, primer and probe sequences used for RT-PCR detection.

Gene	Sequence (5` to 3`)
U6 (RT)	GTCGTATCCAGTGCAGGGTCCGAGGTATTCGCACTGGATACGACAAAAATATG
U6 (F)	CTCGCTTCGGCAGCACA
U6 (R)	AACGCTTCACGAATTTGCGT
miR-486-5p (RT)	GTCGTATCCAGTGCAGGGTCCGAGGTATTCGCACTGGATACGACCTCGGG
miR-486-5p (F)	CACGCATCCTGTACTGAGCTG
miR-486-5p(R)	CAGTGCAGGGTCCGAGGTA
miR-486-3p(RT)	GTCGTATCCAGTGCAGGGTCCGAGGTATTCGCACTGGATACGACTATCCTGT
miR-486-3p(F)	GATCACACGGGGCAGCTCAGTA
miR-486-3p(R)	CAGTGCAGGGTCCGAGGTA
miRNA complementary specific sequences are underlined	

2.4 Western Blot

Western blotting was performed according to standard methods as described previously [52, 53]. Cells were lysed with RIPA buffer (Sigma-Aldrich) supplemented with Protease and Phosphatase Inhibitor (Roche). If

needed, cytoplasmic and nuclear proteins were separated using the NE-PER Nuclear and Cytoplasmic Extraction Reagents (Thermo Fisher Scientific). Protein quantification was performed using BCA Protein Assay Kit (Beyotime, China) and later was denatured and reduced incubating the samples with 5× Dual Color SDS-PAGE Protein Sample Loading Buffer (Beyotime, China) for 30 min at room temperature (15 min at 65 ℃). Equal amounts of proteins were loaded in SDS-PAGE (sodium dodecyl sulfate-polyacrylamide gel electrophoresis gel) NuPAGE™ 10% Bis-Tris Protein Gels (Thermo Fisher Scientific) along with molecular weight marker. Sixty to eighty micrograms of total protein were loaded and transferred onto nitrocellulose membranes (Bio-Rad Laboratories). After blocking in 5% milk and 0.01% Tween-20/PBS for 2 h, membranes were incubated with primary antibodies (Supplementary Table 3) overnight and then with horseradish peroxidase-conjugated (ZS-BIO) secondary antibodies for 2 h. Specific signals of the membranes were analyzed using an ECL detection system (Millipore, Billerica, MA, USA). Actin or Gapdh (Glyceraldehyde-3-phosphate dehydrogenase) was used as a loading control. All experiments were repeated for three times. For quantification, the grey density of the target bands in the immunoblot was analyzed by Image J software (National Institutes of Health, Bethesda, Maryland, U.S.) and normalized to the grey density of β-actin or Gapdh. The following antibodies were used: rabbit anti-β-actin (sc-1616-R; Santa Cruz Biotechnology, Inc.); rabbit anti-phospho-Akt (Ser473) (#4060, Cell Signaling Technology); rabbit anti-Akt (#4691, Cell Signaling Technology); rabbit anti-phospho-P44/42 MAPK (Erk1/2) (Thr202/Tyr204) (#4370, Cell Signaling Technology); rabbit anti- MAPK (Erk1/2) (#4369, Cell Signaling Technology); Secondary antibodies were Horseradish peroxidase (HRP)-conjugated anti-mouse IgG (ZB-2305, ZSGB-Bio) or anti-Rabbit IgG(Fc) (ZB-2301, ZSGB-Bio).

2.5 Statistical Analysis

All statistical analyses were performed using GraphPad Prism 8.3.0 (GraphPad Software). All p values were calculated by a two-tailed Student's t test to test the null hypothesis of no difference between the two compared groups. The assumption of equal variances was tested by an F test. $p < 0.05$ was considered statistically significant. Data are presented as mean ± SEM.

3 Results and Analysis

3.1 Construction of Overexpression and Interference Vectors for mmu-miR-486-5p

We designed oligonucleotide sequence overexpression and interference vectors for mmu-miR-486-5p, which were synthesized by General Biological System (Anhui) Co., Ltd., based on miR-30, miR-451 and miRNA sponge (Table 1). The vector for anti-miR-486-5p TuD (Figure 3B) was established using the oligonucleotide sequence of TuD RNAs (tough decoy RNAs) cloned into the lentivirus plasmid backbone (Figure 3A). Subsequently, the anti-miR-486-5p TuD vector was acquired and analyzed by PCR and DNA sequencing (Figure 3B and 3F). The vector for the anti-miR-486-5p sponge (Figure 3C) was established using the oligonucleotide sequence of six tandem "bulged" miR-486-5p-binding motifs cloned into the lentivirus plasmid backbone (Figure 3A), and then the vector of the anti-miR-486-5p sponge was analyzed by PCR and DNA sequencing (Figure 3C and 3F). Similarly, the vector of miR-486-5p-shRNA30 (Figure 3D) created through the oligonucleotide sequence of miR-30 short hairpin RNA (shRNA) cassettes containing mature miR-486-5p sequences was cloned into the lentivirus plasmid backbone (Figure 3A). Consequently, the miR-486-5p-shRNA30 vector was analyzed by PCR and DNA sequencing (Figure 3D and 3F). Additionally, the vector of miR-486-5p-shRNA451 (Figure 3E) created through the oligonucleotide sequence of miR-451 short hairpin RNA (shRNA) cassettes containing mature miR-486-5p sequences was cloned into the lentivirus plasmid backbone (Figure 3A). Afterward, the miR-486-5p-shRNA451 vector was acquired and analyzed by PCR and DNA sequencing (Figure 3E and 3F). The lentivirus plasmid backbone (PLV-U6-MCS) was used as a control vector. All vectors that were determined to be DNA fragments longer than 300 bp (Figure 3F) containing the target gene sequences, assessed by PCR analysis, were deemed positive clone vectors, and the positive clone vectors were further validated through DNA sequencing (Figure 3B to 3D) to confirm that they were correctly acquired. In summary, these results show that all vectors were constructed successfully, which were then used for all subsequent experiments in this study.

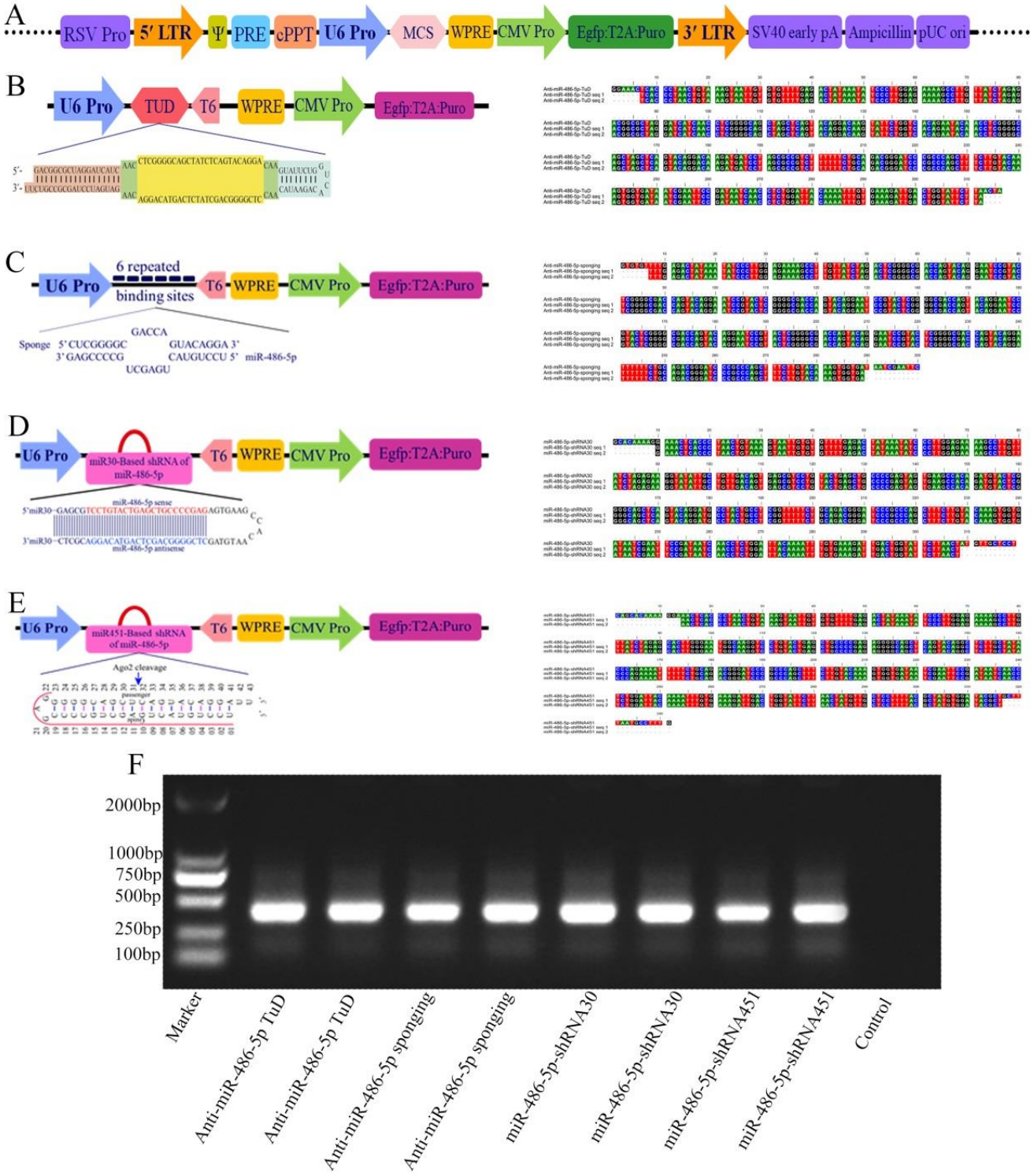

Figure 3 The depiction of the structures of the overexpression and interference vectors of mmu-miR-486-5p and the PCR detection and DNA sequencing results of the constructed vectors.

A The original structure diagram of lentivirus vector backbone. B The main structure and sequencing results of the anti-miR-486-5p TuD vector. C The main structure and sequencing results of the anti-miR-486-5p sponge vector. D The main structure and sequencing results of the anti-miR-486-5p-shRNA30 vector. E The main structure and sequencing results of the anti-miR-486-5p-shRNA451 vector. F The positive clones of all vectors were confirmed by PCR analysis in *Escherichia coli* DH5α. Lane 1: Marker, lane 2–3: positive clone of the anti-miR-486-5p TuD vector, lane 4–5: positive clone of the anti-miR-486-5p sponge vector, lane 6–7: positive clone of the anti-miR-486-5p-shRNA30 vector, lane 8–9: positive clone of the anti-miR-486-5p-shRNA451 vector, lane 10: negative control.

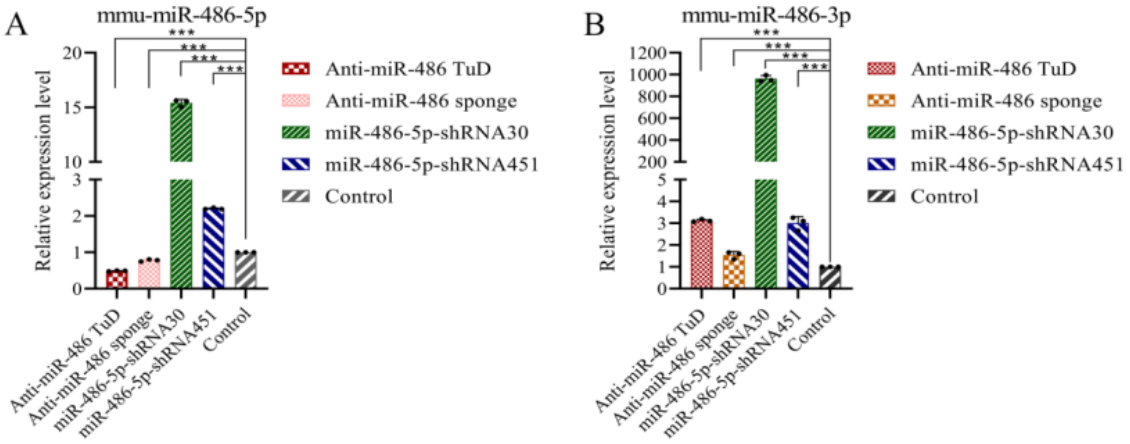

Figure 4 mmu-miR-486-5p and mmu-miR-486-3p expression were assessed by qRT-PCR.

A The C2C12 cells were transduced with anti-miR-486-5p TuD, anti-miR-486-5p sponge, miR-486-5p-shRNA30, miR-486-5p-shRNA45 and PLV-U6-MCS, after which total RNA was harvested, and randomly selected mmu-miR-486-5p expression was analyzed by RT-PCR using stem loop PCR primers (N=3). mmu-miR-486-5p expression was calculated as ΔΔCT after normalization to control. B The C2C12 cells were transduced with anti-miR-486-5p TuD, anti-miR-486-5p sponge, miR-486-5p-shRNA30, miR-486-5p-shRNA45 and PLV-U6-MCS, after which total RNA harvested, and randomly selected mmu-miR-486-3p expression was analyzed by RT-PCR using stem loop PCR primers (N=3). mmu-miR-486-3p expression was calculated as ΔΔCT after normalization to control. miR-486-5p RNA levels are expressed as the mean ± SEM of at least three independent experiments normalized to U6 abundance. The P-values were calculated using unpaired Student's t-tests. No, no significance; *P<0.05; **P<0.01; ***P<0.001.

3.2 Relative Expression Levels of mmu-miR-486-5p Were Detected Using Stem Loop PCR Primers and RT-qPCR in C2C12 Cells

Anti-miR-486-5p TuD, anti-miR-486-5p sponge, miR-486-5p-shRNA30, miR-486-5p-shRNA45 and PLV-U6-MCS were packaged into lentiviruses and transfected into C2C12 cells. Following three weeks of puromycin (Puro) selective pressure, stable cell lines were acquired, and consequently, the cells were collected after 72 h to measure mmu-miR-486-5p and mmu-miR-486-3p expression levels using stem loop PCR primers (Table 2) and RT-qPCR. These results were normalized with the internal reference U6 in this section. Compared to that in the control, anti-miR-486-5p TuD and anti-miR-486-5p sponging not only significantly decreased mmu-miR-486-5p expression levels (Figure 4A) by approximately 0.5- and 0.7-fold in C2C12 cells, respectively, but also did not induce high expression of mmu-miR-486-3p (approximately 3-fold, Figure 4B) in C2C12 cells. Comparing the two results, it can be seen that anti-miR-486-5p TuD could exert the best interference effect for mmu-miR-486-5p expression in C2C12 cells. Further analysis showed that miR-486–5p-shRNA30 and miR-486-5p-shRNA451 led to overexpression of mmu-miR-486-3p in C2C12 cells compared with the control group (Figure 4A). We found that miR-486-5p-shRNA30 upregulated mmu-miR-486-5p expression almost 15-fold (Figure 4A) compared to the control group and that miR-486-5p-shRNA451 only increased mmu-miR-486-5p expression approximately 3-fold (Figure 4A) versus the control group in C2C12 cells. However, miR-486-5p-shRNA30 significantly increased the relative expression of mmu-miR-486-3p to approximately 1000-fold (Figure 4B) in C2C12 cells, and miR-486-5p-shRNA451 only upregulated its expression 3-fold (Figure 4B). miR-486-5p-shRNA451 showed a better result in upregulating mmu-miR-486-5p expression in C2C12 cells when comparing these two sets of data. Overall, these results indicate that we successfully constructed overexpression and interference vectors of mmu-miR-486-5p.

3.3 Validation of mmu-miR-486-5p Function in C2C12 Cells

It is well documented that the expression of p-ERK and p-AKT was remarkably downregulated by overexpression of mmu-miR-486-5p and was notably upregulated through knockdown of mmu-miR-486-5p in a human thyroid epithelial cell line [12]. Additionally, a negative

correlation between mmu-miR-486-5p and its target gene expression, such as Snail, has been demonstrated in cells [14]. Cells that stably expressed miR-486-5p shRNA or siRNA were collected after 72 h to assess protein expression levels via western blots. To further explore the molecular mechanisms of miR-486-5p and prove whether the overexpression and interference vectors of mmu-miR-486-5p were successfully constructed compared with the control group transfected with the PLV-U6-MCS lentivirus, we evaluated the possibility that miR-486-5p contributes to the expression level of Snail, ERK1/2, p-ERK1/2, AKT and p-Akt in C2C12 cells. The western blot results (Figure 5 and Figure 6A) suggested that Snail, p-Akt and p-ERK1/2 were decreased in miR-486-5p-overexpressing C2C12 cells and increased in miR-486-5p-knockdown C2C12 cells. These results are similar to those reported previously in the literature. Interestingly, we also found that ERK1/2 and AKT were nearly downregulated (Figure 5 and Figure 6A) in miR-486-5p-overexpressing C2C12 cells and practically upregulated (Figure 5 and Figure 6A) in miR-486-5p-knockdown C2C12 cells.

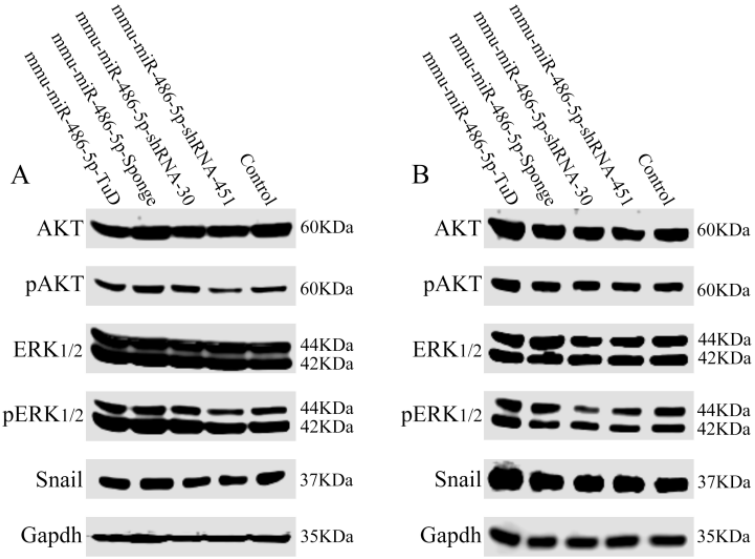

Figure 5 mmu-miR-486-5p regulated protein expression level was analyzed using western blot

cells which could stably express of miR-486-5p shRNA or siRNA were collected after 72h, and lysed to extract total proteins, and then western blot assay was performed to detect changes protein expression of AKT, p-Akt, ERK1/2, p-ERK1/2, Snail and Gapdh, and Gapdh was used as internal reference gene. A and B western blot detected changes protein expression of AKT, p-Akt, ERK1/2, p-ERK1/2, Snail and Gapdh.

To further confirm our results outlined above, statistical grayscale analysis of the western blot bands was performed by ImageJ, using normalization to Gapdh expression in this section. AKT protein expression level was upregulated approximately 1.235-fold and 1.043-fold (Figure 6B) in anti-miR-486-5p TuD and anti-miR-486-5p sponge cells compared with the control group, respectively. The AKT protein expression level was downregulated approximately 0.964-fold and 0.922-fold (Figure 6B) in anti-miR-486-5p-shRNA30 and anti-miR-486-5p-shRNA451 cells compared with the control group, respectively. In addition, the p-AKT protein expression level was upregulated approximately 1.331-fold and 1.098-fold (Figure 6C) in anti-miR-486-5p TuD and anti-miR-486-5p sponge cells compared with the control group, respectively. The p-AKT protein expression level was downregulated approximately 0.775-fold and 0.724-fold (Figure 6C) in anti-miR-486-5p-shRNA30 and anti-miR-486-5p-shRNA451 cells compared with the control group, respectively. Consistently, the ERK1/2 protein expression level was upregulated approximately 1.203-fold and 1.201-fold (Figure 6D) in anti-miR-486-5p TuD and anti-miR-486-5p sponge cells compared with the control group, respectively. The ERK1/2 protein expression level was downregulated approximately 0.788-fold and 0.748-fold (Figure 6D) in anti-miR-486-5p-shRNA30 and anti-miR-486-5p-shRNA451 cells compared with the control group, respectively. Additionally, the p-ERK1/2 protein expression level was upregulated approximately 1.295-fold and 1.186-fold (Figure 6E) in anti-miR-486-5p TuD and anti-miR-486-5p sponge cells

compared with the control group, respectively. The p-ERK1/2 protein expression level was downregulated approximately 0.631-fold and 0.752-fold (Figure 6E) in anti-miR-486-5p-shRNA30 and anti-miR-486-5p-shRNA451 cells compared with the control group, respectively. Subsequently, the Snail protein expression level was upregulated approximately 1.304-fold and 1.181-fold (Figure 6F) in anti-miR-486-5p TuD and anti-miR-486-5p sponge cells compared with the control group, respectively. Snail protein expression level was downregulated approximately 0.848-fold and 0.792-fold (Figure 6F) in anti-miR-486-5p-shRNA30 and anti-miR-486-5p-shRNA451 cells compared with the control group, respectively. Taken together, these results indicated that we successfully constructed shRNA/siRNA lentiviral expression vectors for microRNA-486-5p.

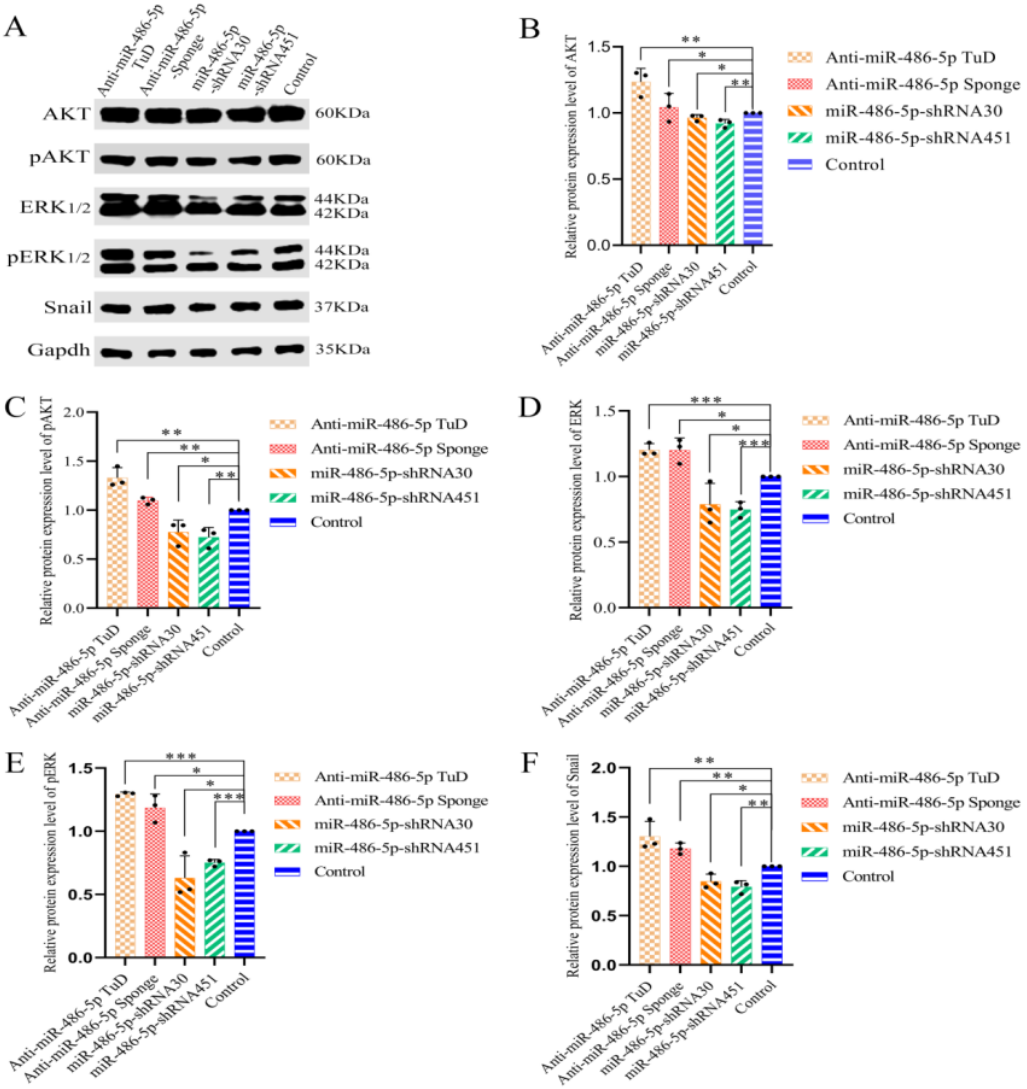

Figure 6 mmu-miR-486-5p-regulated protein expression levels were analyzed using western blotting and ImageJ

Cells that could stably express miR-486-5p shRNA or siRNA were collected after 72 h and lysed to extract total proteins, after which a western blot assay was performed to detect changes in the protein expression of AKT, p-Akt, ERK1/2, p-ERK1/2, Snail and Gapdh, with Gapdh used as the internal reference gene. A Western blot results demonstrated changes in the protein expression of AKT, p-Akt, ERK1/2, p-ERK1/2, Snail and Gapdh. All western blot results underwent gray level analysis of the western blot bands by ImageJ software, with Gapdh expression used for normalization. B Relative protein expression level of AKT was calculated by comparing to the control group. C Relative protein expression level of p-AKT was calculated by comparing to the control group. D Relative protein expression level of ERK1/2 was calculated by comparing to the control group. E Relative protein expression level of p-ERK1/2 was calculated by comparing to the control group. F Relative protein expression level of Snail was calculated by comparing to the control group. All data are shown as the means ± S.D. of at least three independent experiments. The P-values were calculated using unpaired Student's t-tests. No, no significance; *P<0.05; **P<0.01; ***P<0.005.

4 Discussion

Growing evidence has recently revealed that miRNA mimics (agomiR) and miRNA inhibitors (antagomiR) [54-56], which have the disadvantages of a short induction time, low transfection efficiency, high cost and unfavorability for building stable cell lines compared with lentivirus expression vectors, have been used to study the biological functions of miRNA. The rare phenomenon was found that the mature 5p sequence of miRNA had complementary pairing with the mature 3p sequences of miRNA, such as in miR-486 (Figure 1) [7, 9], which presents an issue for establishing lentiviral vectors expressing mmu-miR-486-5p. Based on the development of the canonical and noncanonical biogenesis pathways of miRNAs, it has been shown that the Dicer-independent miRNA biogenesis pathway involves the unusually short hairpin of miR-451 [22-24] and that the canonical miRNA biogenesis pathway contains the commonly short hairpin of miR-30 [15, 25], providing a method to construct lentiviral vectors overexpressing mmu-miR-486-5p. Currently, short hairpin RNA (shRNA) molecule cassettes containing miRNA mature sequences have been designed based on the structure of miR-30 and miR-451 [15, 25, 26] for overexpression of miRNA, such as miR-451 [26], miR-30 [15], and miR-130a-3p [57]. Based on these principles, we successfully constructed lentiviral overexpression vectors of mmu-miR-486-5p, miR-486-5p-shRNA30 and miR-486-5p-shRNA45. Both lentiviral overexpression vectors could increase mmu-miR-486-5p expression (Figure 4A) in C2C12 cells, but mmu-miR-486-3p was increased almost 1000-fold (Figure 4B) in miR-486-5p-shRNA30 C2C12 cells, and there was an approximately 3-fold increase (Figure 4B) in miR-486-5p-shRNA451 C2C12 cells. In addition, based on developments in the inhibition of miRNA function, sponges (such as six repeated binding sites) and decoy RNA molecules (TuD RNAs (tough decoy RNAs)), which contain miRNA antisense oligonucleotide sequences, were also constructed as lentiviral overexpression vectors for interference or knockdown of miRNA expression in vivo [32-35, 40]. Jun Xie et al [37] showed that recombinant adeno-associated virus vectors combined with TuDs are more effective than sponges or miRZips at inhibiting miR-122 or specific miRNA expression and function in vivo. Based on this fundamental idea, we successfully constructed lentiviral interference vectors for mmu-miR-486-5p, anti-miR-486-5p TuD and anti-miR-486-5p sponge. Both lentiviral interference vectors not only downregulated mmu-miR-486-5p expression (Figure 4A) but also did not induce high expression of mmu-miR-486-3p (Figure 4B) in C2C12 cells. The results, which were consistent with previous research, showed that anti-miR-486-5p TuD was more effective than the anti-miR-486-5p sponge at reducing mmu-miR-486-5p expression (Figure 4A) in vivo. Overall, the above results showed that the lentivirus expression vector mmu-miR-486-5p was successfully constructed.

The canonical miRNA function is to repress the expression of target genes at the transcriptional and/or posttranscriptional levels by directly binding the 3'UTR of target mRNAs [58-60], especially for negatively modulating protein expression levels in vivo. Recent literature [12] has indicated that in papillary thyroid carcinoma cells, miR-486-5p mimics significantly downregulate p-AKT and p-ERK expression and miR-486-5p inhibition notably upregulates p-AKT and p-ERK expression. We also obtained similar results (Figure 6A, 6C, 6E and Figure 5) using western blots and ImageJ, which showed that p-AKT and p-ERK expression was diminished in C2C12 cells that were treated with miR-486-5p-shRNA30 and miR-486-5p-shRNA45 and enhanced in C2C12 cells that were treated with anti-miR-486-5p TuD and anti-miR-486-5p sponge. Moreover, Xiaoguang Zhang et al [14] demonstrated that miR-486-5p inhibits prostate cancer (PCa) cell migration, invasion and epithelial–mesenchymal transition by negatively regulating Snail protein expression and that Snail expression is decreased or increased, respectively, in miR-486-5p-overexpressing or miR-486-5p-inhibited PCa cells. In our western blot and ImageJ analyses, Snail expression (Figure 6A, 6F and Figure 5) was also attenuated in miR-486-5p-shRNA30- and miR-486-5p-shRNA45-infected C2C12 cells and augmented in anti-miR-486-5p TuD- and anti-miR-486-5p sponge-infected C2C12 cells. Moreover, we further explored AKT and ERK expression in C2Cl2 cells infected with all lentivirus expression vectors. AKT and ERK expression (Figure 6A, 6B, 6D and Figure 5) was ameliorated in anti-miR-486-5p TuD- and anti-miR-486-5p sponge-infected C2C12 cells and restrained in miR-486-5p-shRNA30- and miR-486-5p-shRNA45-infected C2C12 cells. On the basis of these results, we hypothesize that mmu-miR-486-5p can directly regulate the AKT and ERK1/2 signaling

pathways to affect C2C12 cell development. Of course, this conjecture needs to be confirmed by further experimental data or results in the future. Based on these results, the biological function of mmu-miR-486-5p remains constant, with canonical miRNA functions that negatively regulate protein expression levels in vivo. In terms of functional aspects of miRNA, we further proved that the mmu-miR-486-5p lentivirus expression vector can exert the canonical miRNA function of inversely modulating protein expression levels in C2C12 cells.

In summary, we successfully established shRNA (miR-486-5p-shRNA30 and miR-486-5p-shRNA45) and siRNA (anti-miR-486-5p TuD and anti-miR-486-5p sponge) lentiviral expression vectors for mi-croRNA-486-5p based on miR-30/451 and miRNA sponges. These results proved that anti-miR-486-5p TuD and miR-486-5p-shRNA451, which did not cause the substantial expression of miR-486-3p and remarkably upregulated and downregulated protein expression levels (AKT and pAKT, ERK1/2 and pERK1/2, and Snail) in C2C12 cells, were superior to the anti-miR-486-5p sponge and miR-486-5p-shRNA30. Anti-miR-486-5p TuD and miR-486-5p-shRNA451 provide simple ways to build long-term effective overexpression or interference of mmu-miR-486-5p in C2C12 and mice, to study miRNA function in C2C12 or mice, and to serve as a potential new diagnostic method for diseases caused by miRNA deregulation.

Conflicts of Interest

The authors declare no conflict of interest.

References

[1] KIM V N, HAN J, SIOMI M C. Biogenesis of small RNAs in animals [J]. Nat Rev Mol Cell Biol, 2009, 10(2): 126-139.

[2] KROL J, LOEDIGE I, FILIPOWICZ W. The widespread regulation of microRNA biogenesis, function and decay [J]. Nat Rev Genet, 2010, 11(9): 597-610.

[3] PRITCHARD C C, CHENG H H, TEWARI M. MicroRNA profiling: approaches and considerations [J]. Nat Rev Genet, 2012, 13(5): 358-369.

[4] DEVEALE B, SWINDLEHURST-CHAN J, BLELLOCH R. The roles of microRNAs in mouse development [J]. Nat Rev Genet, 2021, 22(5): 307-323.

[5] DRAGOMIR M P, KNUTSEN E, CALIN G A. SnapShot: Unconventional miRNA Functions [J]. Cell, 2018, 174(4): 1038-1038 e1031.

[6] KOZOMARA A, BIRGAOANU M, GRIFFITHS-JONES S. miRBase: from microRNA sequences to function [J]. Nucleic acids research, 2019, 47(D1): D155-D162.

[7] ELKHOULY A M, YOUNESS R A, GAD M Z. MicroRNA-486-5p and microRNA-486-3p: Multifaceted pleiotropic mediators in oncological and non-oncological conditions [J]. Non-coding RNA research, 2020, 5(1): 11-21.

[8] ALEXANDER M S, CASAR J C, MOTOHASHI N, et al. Regulation of DMD pathology by an ankyrin-encoded miRNA [J]. Skeletal muscle, 2011, 1(27): 1-17.

[9] SMALL E M, O'ROURKE J R, MORESI V, et al. Regulation of PI3-kinase/Akt signaling by muscle-enriched microRNA-486 [J]. Proceedings of the National Academy of Sciences of the United States of America, 2010, 107(9): 4218-4223.

[10] SHENOY A, BLELLOCH R H. Regulation of microRNA function in somatic stem cell proliferation and differentiation [J]. Nat Rev Mol Cell Biol, 2014, 15(9): 565-576.

[11] ALEXANDER M S, CASAR J C, MOTOHASHI N, et al. MicroRNA-486-dependent modulation of DOCK3/PTEN/AKT signaling pathways improves muscular dystrophy-associated symptoms [J]. J Clin Invest, 2014, 124(6): 2651-2667.

[12] SUN Y H, LIU Z F, YANG B B, et al. MicroRNA-486 inhibits cell proliferation, invasion and migration via down-regulating the TENM1 expressions and affecting ERK and Akt signaling pathways and epithelial-to-mesenchymal transition in papillary thyroid carcinoma [J]. Eur Rev Med Pharmacol Sci, 2019, 23(19): 8429-8439.

[13] WANG A, ZHU J, LI J, et al. Downregulation of KIAA1199 by miR-486-5p suppresses tumorigenesis in lung cancer [J]. Cancer medicine, 2020, 9(15): 5570-5586.

[14] ZHANG X, ZHANG T, YANG K, et al. miR-486-5p suppresses prostate cancer metastasis by targeting Snail and regulating epithelial-mesenchymal transition [J]. OncoTargets and therapy, 2016, 2016(9): 6909-6914.

[15] CHANG K, MARRAN K, VALENTINE A, et al. Creating an miR30-based shRNA vector [J]. Cold Spring Harb Protoc, 2013, 2013(7): 631-635.

[16] DOW L E, PREMSRIRUT P K, ZUBER J, et al. A pipeline for the generation of shRNA transgenic mice [J]. Nat Protoc, 2012, 7(2): 374-393.

[17] CHANG K, ELLEDGE S J, HANNON G J. Lessons from Nature: microRNA-based shRNA libraries [J]. Nat Methods, 2006, 3(9): 707-714.

[18] CHEUNG T H, QUACH N L, CHARVILLE G W, et al. Maintenance of muscle stem-cell quiescence by microRNA-489 [J]. Nature, 2012, 482(7386): 524-528.

[19] TREIBER T, TREIBER N, MEISTER G. Regulation of microRNA biogenesis and its crosstalk with other cellular pathways [J]. Nat Rev Mol Cell Biol, 2019, 20(1): 5-20.

[20] MIYOSHI K, MIYOSHI T, SIOMI H. Many ways to generate microRNA-like small RNAs: non-canonical pathways for microRNA production [J]. Mol Genet Genomics, 2010, 284(2): 95-103.

[21] BARTEL D P. Metazoan MicroRNAs [J]. Cell, 2018, 173(1): 20-51.

[22] CIFUENTES D, XUE H, TAYLOR D W, et al. A novel miRNA processing pathway independent of Dicer requires Argonaute2 catalytic activity [J]. Science, 2010, 328(5986): 1694-1698.

[23] YANG J S, MAURIN T, ROBINE N, et al. Conserved vertebrate mir-451 provides a platform for Dicer-independent, Ago2-mediated microRNA biogenesis [J]. Proceedings of the National Academy of Sciences of the United States of America, 2010, 107(34): 15163-15168.

[24] CHELOUFI S, DOS SANTOS C O, CHONG M M, et al. A dicer-independent miRNA biogenesis pathway that requires Ago catalysis [J]. Nature, 2010, 465(7298): 584-589.

[25] BOFILL-DE ROS X, GU S. Guidelines for the optimal design of miRNA-based shRNAs [J]. Methods, 2016, 103(157-166.

[26] HERRERA-CARRILLO E, BERKHOUT B. Dicer-independent processing of small RNA duplexes: mechanistic insights and applications [J]. Nucleic acids research, 2017, 45(18): 10369-10379.

[27] HERRERA-CARRILLO E, HARWIG A, BERKHOUT B. Silencing of HIV-1 by AgoshRNA molecules [J]. Gene Ther, 2017, 24(8): 453-461.

[28] HARWIG A, KRUIZE Z, YANG Z, et al. Analysis of AgoshRNA maturation and loading into Ago2 [J]. PloS one, 2017, 12(8): 1-15.

[29] SHANG R, ZHANG F, XU B, et al. Ribozyme-enhanced single-stranded Ago2-processed interfering RNA triggers efficient gene silencing with fewer off-target effects [J]. Nature communications, 2015, 6(2014): 8430-8443.

[30] HARWIG A, HERRERA-CARRILLO E, JONGEJAN A, et al. Deep Sequence Analysis of AgoshRNA Processing Reveals 3' A Addition and Trimming [J]. Molecular therapy Nucleic acids, 2015, 4(2015): e247-e255.

[31] LIU Y P, SCHOPMAN N C, BERKHOUT B. Dicer-independent processing of short hairpin RNAs [J]. Nucleic acids research, 2013, 41(6): 3723-3733.

[32] SONG L, LIN C, GONG H, et al. miR-486 sustains NF-kappaB activity by disrupting multiple NF-kappaB-negative feedback loops [J]. Cell research, 2013, 23(2): 274-289.

[33] MOCKENHAUPT S, GROSSE S, RUPP D, et al. Alleviation of off-target effects from vector-encoded shRNAs via codelivered RNA decoys [J]. Proceedings of the National Academy of Sciences of the United States of America, 2015, 112(30): E4007-4016.

[34] HARAGUCHI T, OZAKI Y, IBA H. Vectors expressing efficient RNA decoys achieve the long-term suppression of specific microRNA activity in mammalian cells [J]. Nucleic acids research, 2009, 37(6): e43-e56.

[35] CAO H, YU W, LI X, et al. A new plasmid-based microRNA inhibitor system that inhibits microRNA families in transgenic mice and cells: a potential new therapeutic reagent [J]. Gene Ther, 2016, 23(6): 527-542.

[36] ZAHM A M, MENARD-KATCHER C, BENITEZ A J, et al. Pediatric eosinophilic esophagitis is associated with changes in esophageal microRNAs [J]. Am J Physiol Gastrointest Liver Physiol, 2014, 307(8): G803-G812.

[37] XIE J, AMERES S L, FRIEDLINE R, et al. Long-term, efficient inhibition of microRNA function in mice using rAAV vectors [J]. Nature methods, 2012, 9(4): 403-409.

[38] GOU D, ZHANG H, BAVISKAR P S, et al. Primer extension-based method for the generation of a siRNA/miRNA expression vector [J]. Physiol Genomics, 2007, 31(3): 554-562.

[39] LIU Y P, KARG M, HERRERA-CARRILLO E, et al. Towards Antiviral shRNAs Based on the AgoshRNA Design [J]. PloS one, 2015, 10(6): e0128618.

[40] GENTNER B, SCHIRA G, GIUSTACCHINI A, et al. Stable knockdown of microRNA in vivo by lentiviral vectors [J]. Nat Methods, 2009, 6(1): 63-66.

[41] TISCORNIA G, SINGER O, VERMA I M. Design and cloning of lentiviral vectors expressing small interfering RNAs [J]. Nat Protoc, 2006, 1(1): 234-240.

[42] QIU H, ZHONG J, LUO L, et al. A PCR-Based Method to Construct Lentiviral Vector Expressing Double Tough Decoy for miRNA Inhibition [J]. PloS one, 2015, 10(12): e0143864.

[43] MATVEEVA O V, NAZIPOVA N N, OGURTSOV A Y, et al. Optimized models for design of efficient miR30-based shRNAs [J]. Frontiers in genetics, 2012, 3(163): 1-12.

[44] ELEGHEERT J, BEHIELS E, BISHOP B, et al. Lentiviral transduction of mammalian cells for fast, scalable and high-level production of soluble and membrane proteins [J]. Nat Protoc, 2018, 13(12): 2991-3017.

[45] SINGER O, TISCORNIA G, IKAWA M, et al. Rapid generation of knockdown transgenic mice by silencing lentiviral vectors [J]. Nat Protoc, 2006, 1(1): 286-292.

[46] LESCH H P, LAITINEN A, PEIXOTO C, et al. Production and purification of lentiviral vectors generated in 293T suspension cells with baculoviral vectors [J]. Gene Ther, 2011, 18(6): 531-538.

[47] TISCORNIA G, SINGER O, VERMA I M. Production and purification of lentiviral vectors [J]. Nat Protoc, 2006, 1(1): 241-245.

[48] LALIT P A, RODRIGUEZ A M, DOWNS K M, et al. Generation of multipotent induced cardiac progenitor cells from mouse fibroblasts and potency testing in ex vivo mouse embryos [J]. Nat Protoc, 2017, 12(5): 1029-1054.

[49] SUN N, LEE A, WU J C. Long term non-invasive imaging of embryonic stem cells using reporter genes [J]. Nat Protoc, 2009, 4(8): 1192-1201.

[50] RICHNER M, VICTOR M B, LIU Y, et al. MicroRNA-based conversion of human fibroblasts into striatal medium spiny neurons [J]. Nat Protoc, 2015, 10(10): 1543-1555.

[51] KRAMER M F. Stem-loop RT-qPCR for miRNAs [J]. Curr Protoc Mol Biol, 2011, Chapter 15(10): 151000-151015.

[52] MOSER J J, CHAN E K, FRITZLER M J. Optimization of immunoprecipitation-western blot analysis in detecting GW182-associated components of GW/P bodies [J]. Nat Protoc, 2009, 4(5): 674-685.

[53] GIRARDI F, TALEB A, EBRAHIMI M, et al. TGFbeta signaling curbs cell fusion and muscle regeneration [J]. Nature communications, 2021, 12(1): 750-766.

[54] STEINKRAUS B R, TOEGEL M, FULGA T A. Tiny giants of gene regulation: experimental strategies for microRNA functional studies [J]. Wiley Interdiscip Rev Dev Biol, 2016, 5(3): 311-362.

[55] HENSHALL D C, HAMER H M, PASTERKAMP R J, et al. MicroRNAs in epilepsy: pathophysiology and clinical utility [J]. Lancet Neurol, 2016, 15(13): 1368-1376.

[56] LU T X, ROTHENBERG M E. MicroRNA [J]. J Allergy Clin Immunol, 2018, 141(4): 1202-1207.

[57] ZHAO J, WANG H, ZHOU J, et al. miR-130a-3p, a Preclinical Therapeutic Target for Crohn's Disease [J]. J Crohns Colitis, 2021, 15(4): 647-664.

[58] LIN S, GREGORY R I. MicroRNA biogenesis pathways in cancer [J]. Nature reviews Cancer, 2015, 15(6): 321-333.

[59] MICHLEWSKI G, CACERES J F. Post-transcriptional control of miRNA biogenesis [J]. Rna, 2019, 25(1): 1-16.

[60] ZHANG S, LIU Y, YU B. New insights into pri-miRNA processing and accumulation in plants [J]. Wiley Interdiscip Rev RNA, 2015, 6(5): 533-545.